Improving Aluminum Resistance Spot Welding in Automotive Structures

The fabrication process in producing the 2014 Corvette Stingray uses the Multi-Ring Domed electrode patented by General Motors (GM). A — Welding this Corvette's space frame; B — weld spots on the space frame; C — the space frame; and D — body structure. (Photos courtesy of GM.)

A

B

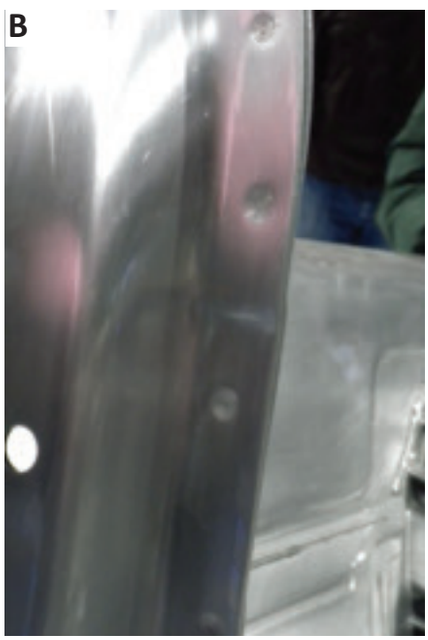

C

D

BY DAVID R. SIGLER, BLAIR E. CARLSON, AND PAUL JANIAK

*DAVID R. SIGLER (*david.r.sigler@gm.com*) and BLAIR E. CARLSON are with the General Motors Global Research and Development Center, Warren, Mich. PAUL JANIAK is with Swerea KIMAB AB, Stockholm, Sweden.*

Based on a presentation at the AWS Detroit Section's Sheet Metal Welding Conference XV held October 2–5, 2012, in Livonia, Mich.

A recently developed electrode design features multiple protruding rings that penetrate oxide layers by straining the aluminum sheet surface during welding

The majority of automotive body shop welding consists of resistance spot welding (RSW) steel sheet due to its inherently low cost and high speed. With the introduction of aluminum, it is desirable to continue using RSW as the joining process. However, the presence of insulating oxide layers on the aluminum alloy material surface presents significant problems in obtaining consistent spot welding processes.

This problem has been solved by General Motors (GM) with the invention of its patented Multi-Ring Domed (MRD) electrode (Refs. 1, 2). This key process is currently used by the company in automotive structures, such as for the 2014 Corvette Stingray — see lead photos.

The electrode design incorporates several protruding concentric rings on the weld face that act to deform the aluminum sheet surface on contact and break through oxides on the surface, which is essential to obtaining a stable aluminum spot welding process. Developing dressing blades that cut protruding rings into the electrode weld face has been a critical enabler for its introduction into GM plants (Ref. 3).

Weld Face Importance

To ensure a consistent, high-quality welding process, the electrode weld face must not be allowed to experience significant degradation. Also, the weld face requires maintenance by dressing at regular intervals. It is crucial that the dressing frequency and depth of cut be sufficient to maintain the electrode weld face geometry. However, both must not be so aggressive that excessive amounts of material are removed, which would require more frequent electrode changes and higher manufacturing costs.

During aluminum spot welding, damage to the weld face of conventional electrodes occurs primarily by reaction between the copper electrode and aluminum sheet that leads to pit formation on the electrode surface (Ref. 4). In the case of pitting damage where small cavities form in the weld face, complete removal of the pits requires extended dressing, which can significantly shorten electrode life. If dressing fails to completely remove the pits, it will cause the electrode surface to deteriorate more rapidly, which in turn will eventually lead to unacceptable welds.

Macrodeformation of the electrode, which commonly happens in steel spot welding, does not occur for aluminum spot welding because the nugget temperatures are much lower. However, circular protrusions on the MRD electrode with their small cross sections can be susceptible to deformation or flattening during use.

Determining the Electrode's Key Factors

This research evaluated the MRD welding electrode in terms of wear that occurs during spot welding aluminum alloys and developed an understanding of the damage mechanism. Evaluation included assessing both mechanical deformation and weld face erosion due to metallurgical reactions between the copper electrode and aluminum sheet.

A variety of electrode materials with different properties were assessed to identify those properties most important for extending electrode life. This information is key to determining electrode wear rates and establishing the proper dressing frequency and cut depth.

The most commonly used electrode material in GM production facilities is copper-zirconium Alloy C15000. This served as a reference for comparison against four other copper electrode materials selected based on their properties, including hardness, softening temperature, and electrical conductivity.

Wear rates and the associated electrode wear mechanisms were expected to differ as a function of the composition and surface condition of the material to be welded. Therefore, the electrodes in this project were evaluated by welding two different, commonly used aluminum sheet materials — AA5754-O and AA6111-T4.

Research Materials Used

The assessment included five different electrode materials. The most commonly used electrode, Alloy C15000, served as a reference material. Evaluation included welding 2.0-mm AA5754-O and 2.0-mm AA6111-T4 sheets. The two aluminum alloys were welded only to themselves and not to each other. Following welding, the electrodes were analyzed for mechanical deformation and weld face erosion to determine the wear extent and mechanisms.

Electrode Design and Properties

The electrodes used in this project employed GM's patented weld face geometry used for spot welding aluminum (Refs. 1, 2). Incorporating geometric features into the electrode weld face reduces resistance at the electrode/sheet interface and improves heat transfer between the electrode and aluminum sheet during spot welding. These features include protruding circular rings that penetrate through the outer oxide layers of the aluminum sheet by straining the sheet surface during welding (Ref. 2).

Table 1 — Electrode Types and Their Properties

	Resistivity µohm cm	Hardness HV	½ Softening Temperature, 1 h	Nominal Composition %
C15000	1.94	145	550	Zr 0.15
C15760	2.08	160	1000	Al 0.6 as Al_2O_3
C18000	4.31	200	600	Cr 0.45; Ni 2.4; Si 0.6
C18150	2.08	160	600	Cr 1.0; Zr 0.1
X-trode core	2.08	145	1000	Al 0.6 as Al_2O_3
X-trode shell	1.94	130	550	Zr 0.15

Table 2 — Welding Parameters Used for Each Sheet Alloy and Electrode Material

Electrode Alloy	AA6111-T4 Force	AA6111-T4 Current	AA5754-O Force	AA5754-O Current	Weld Time Both Alloys	Hold Time Both Alloys
C15000 (ref)	4.9 kN	27.5 kA	5.35 kN	28.0 kA	150 ms	34 ms
C18150	4.9 kN	29.0 kA	5.35 kN	29.3 kA	150 ms	34 ms
C15760	4.9 kN	29.0 kA	5.35 kN	29.3 kA	150 ms	34 ms
FF19Z02	4.9 kN	29.5 kA	5.35 kN	29.0 kA	150 ms	34 ms
C18000	4.9 kN	27.0 kA	5.35 kN	26.7 kA	150 ms	34 ms

By reducing the interface resistance and improving heat transfer, heat generation at the electrode/sheet interface is minimized, which significantly improves process robustness and eliminates external expulsion events.

As shown in Table 1, selecting the electrode materials was based on a combination of resistivity and potential wear resistance (both initial hardness and half-softening temperature).

Conducting Welding Trials

A robotically controlled medium-frequency inverter DC weld gun, a Matuschek Servo gun C-type with an integrally mounted transformer (222 kVA, 50:1 turns ratio), was used for all welding trials. In addition, primary current was provided by a Matuschek Servo Spatz M800LL inverter weld control.

Each welding trial began with freshly dressed electrodes. Electrode materials were evaluated after a set number of welds (10, 40, and 100 welds). GM recommendations for weld schedules were followed with only minor adjustments to achieve a button diameter of at least 5.5 mm for each electrode and sheet combination. The weld schedules for each electrode material appear in Table 2.

Weld button measurements were completed at Swerea KIMAB by measuring the size of the actual button pulled out. This is in contrast to the approach used by GM (Ref. 5) where the weld size is taken as the size of the fused area at the faying interface. This difference may have resulted in somewhat elevated weld currents to achieve the desired button diameter and somewhat elevated wear rates as compared to a scenario that uses the fused area to establish weld size.

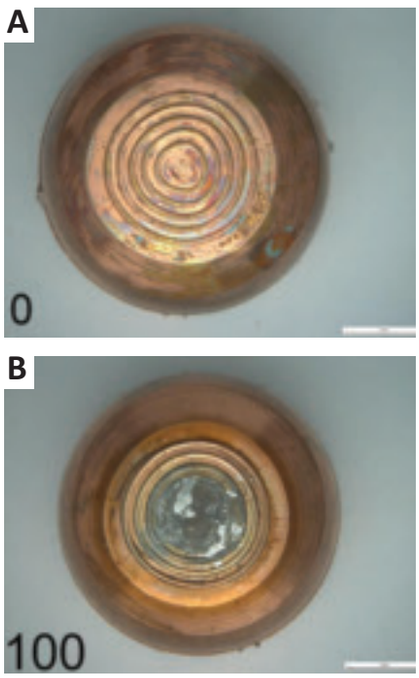

Fig. 1 — The MRD electrode. A — Freshly dressed; and B — after 100 welds.

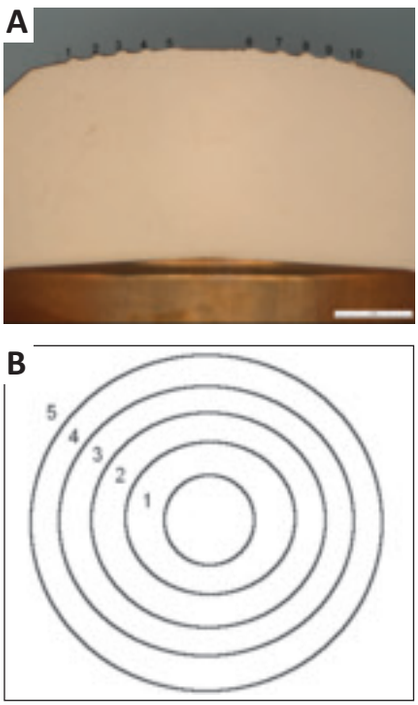

Fig. 2 — Peak numbering system. A — Mounted electrodes; and B — numbering for the weld face rings.

To ensure consistent welding speed and spot spacing, welding trials were done using a robot. A spot spacing of 22 mm was used for all welds. The time interval between consecutive spots is estimated to be ~3 s. Panels having 12 × 5 in. dimensions were used for all trials. This resulted in a maximum of 61 spots per panel.

Study on Electrode Evaluation

Each electrode material was evaluated after welding a set of 10, 40, and 100 spot welds for each sheet material. New

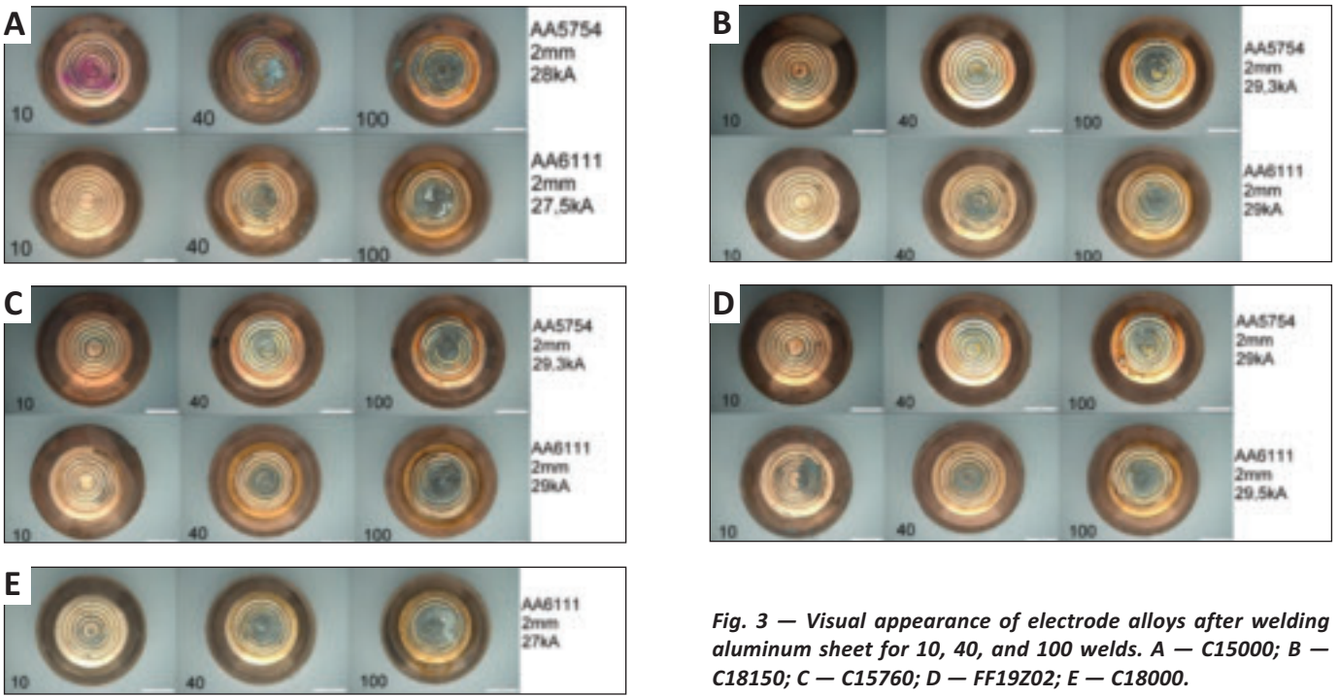

Fig. 3 — Visual appearance of electrode alloys after welding aluminum sheet for 10, 40, and 100 welds. A — C15000; B — C18150; C — C15760; D — FF19Z02; E — C18000.

electrodes were used for each set of welds to evaluate the progression in damage to the electrode surface throughout the whole range of 100 welds.

Light optical microscopy images were taken of all electrodes after welding. Images from each welded combination of electrode and sheet material were compared to qualitatively rank electrodes in terms of resistance to aluminum surface contamination. Figure 1 shows typical optical images of the electrode weld surface after dressing and 100 welds.

To further evaluate wear, the electrodes were cut in half, mounted in conductive filler phenolic mounting compound, ground, polished, and examined. Scanning electron microscope (SEM) evaluation along with energy-dispersive spectroscopy (EDS) analysis was used to measure electrode peak heights and analyze potential buildup of aluminum contamination on the electrode weld face. Initial evaluations showed only minor or no electrode wear after 10 welds, so further evaluation of the electrodes was confined to 40 and 100 welds.

As seen in Fig. 1, the MRD electrode weld face has five protruding rings. Durability of these rings is a primary consideration for electrode life. Due to the radius of curvature of the weld face (25 mm) and electrode design, contact occurs primarily between the two inner rings and sheet during welding. Therefore, the focus of the SEM investigations was on the two innermost rings. Figure 2 illustrates the numbering system used for the rings and peaks.

Visual Appearance of Electrodes after Welding

During welding, the electrode surface gradually reacts with the sheet material and becomes contaminated with aluminum. Visual observation of the electrodes after 10, 40, and 100 spot welds was an attempt to qualitatively rank electrodes in terms of resistance to aluminum contamination on the weld face.

Contamination of the electrode weld face by aluminum modifies the weld face surface properties, i.e., interface electrical resistance and ability to transfer heat. Contamination or metallurgical bonding of aluminum to the copper electrode surface via microwelding creates a more resistive surface. This, in turn, generates more heat at the electrode/sheet interface during welding, which further accelerates electrode degradation.

Aluminum contamination on the copper electrode can sometimes be brittle in nature due to the formation of intermetallic phases between aluminum and copper (Ref. 6). When these intermetallics are subjected to thermal and mechanical stresses during welding, pitting damage can occur on the electrode weld face; for example, the intermetallics pull out of the copper surface leaving a void or pit. The goal is to minimize contamination to increase electrode life and achieve a more stable welding process.

Figure 3A–E are images of all electrode/sheet combinations that were welded together. Table 3 is an attempt to qualitatively rank electrodes in terms of resistance to material buildup.

Ring Wear Review

The MRD electrode features protruding rings on its weld face to penetrate and break up oxide on the sheet surface as well as enable a more stable current transfer into the material during spot welding. In this work, peak height meas-

Table 3 — Ranking of Electrode Performance in Terms of Visual Buildup on the Electrode Surface

Sheet	Least Buildup				Most Buildup
AA5754-O	FF19Z02	C18150	C15000 (ref)	C15760	
AA6111-T4	C15760	FF19Z02	C15000	C15760	C18000

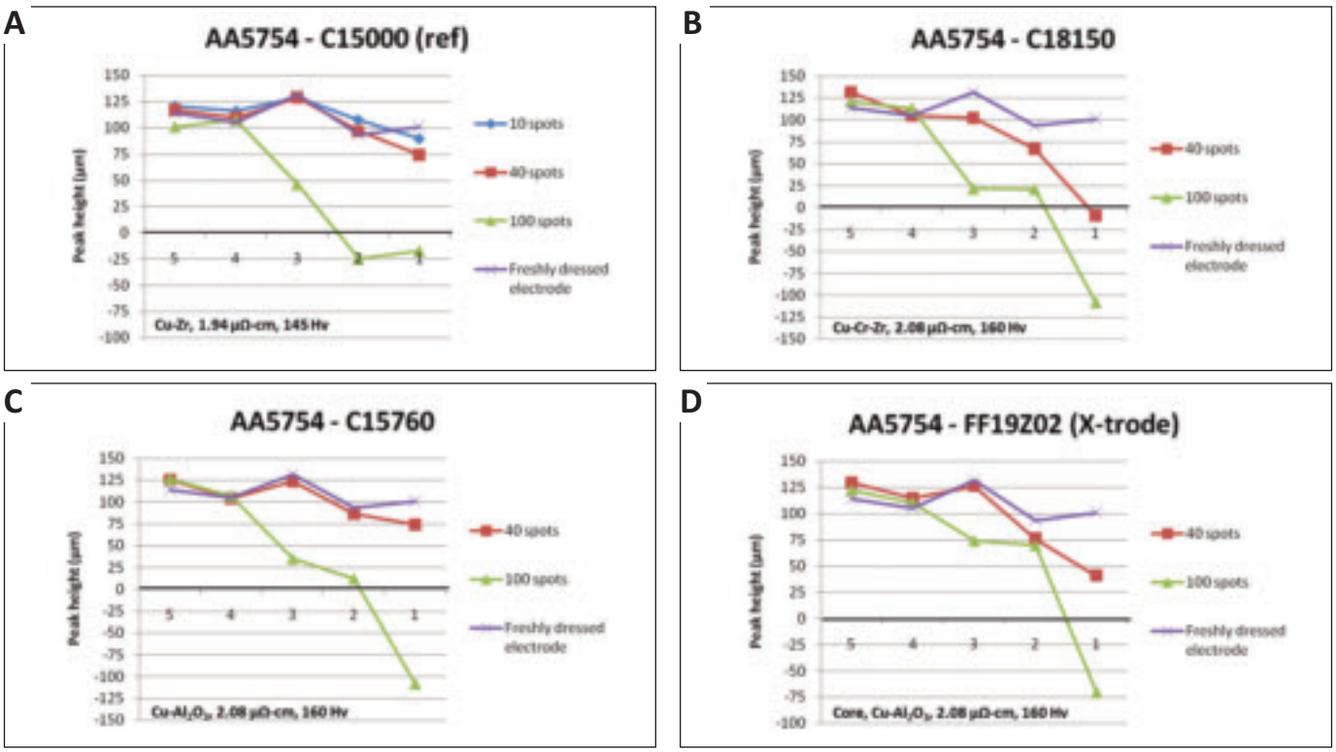

Fig. 4 — Electrode peak height measurements after welding a 2.0-mm, AA5754-O sheet. A — AA5754 – C15000; B — AA5754 – C18150; C — AA5754 – C15760; D — AA5754 – FF19ZO2.

urements on the rings were used to determine wear rates and help understand the mechanisms for electrode degradation.

Ring heights were measured after 10, 40, and 100 welds for each electrode and sheet material combination. Peaks and rings are numbered according to Fig. 2. Results from the wear tests and peak height measurements are presented in Figs. 4 and 5.

The X-axis on the peak height measurement graphs are numbered 1–5 where each number represents the individual rings on the electrode surface according to Fig. 2B where ring number 1 refers to the inner ring. Each ring height value is the average of two different measuring points on a cross section of the electrode. Cutting of the electrodes was performed, keeping the section parallel to the electrode walls, and minimizing any distortion in the ring height measurements.

Figure 4 shows electrode peak height measurements after welding an AA5754-O sheet. The purple line indicates peak heights for the as-dressed electrode. Typical peak height of the as-dressed electrode varied from about 90 to 125 µm. Little wear was noted after 10 welds (see Figs. 4A and 5A blue lines), so additional measurements at this number of welds were discontinued. Wear is noticeable after 40 welds, especially for the C18150 electrode.

Both the C15000 reference electrode and C15760 oxide dispersion strengthened electrode showed good performance out to 40 welds, maintaining fairly good ring height, which will help ensure they establish good contact with the sheet surface.

In all cases at 100 welds, wear of rings 1 and 2 became much more pronounced. At this point, the FF19Z02 electrode showed a fairly good peak height of ~75 microns at ring 2 and 3 locations, whereas the other electrodes showed poorer performance. However, none of the electrodes performed well at this number of welds; either pitting or flattening of one or both inner rings occurred by this point.

Peak height measurements after welding an AA6111-T4 sheet are shown in Fig. 5. For the reference C15000 material, it is apparent that at 40 welds much more wear has occurred, especially for ring 1, when welding AA6111-T4 (Fig. 5A) than when welding AA5754-O (Fig. 4A). The other four electrode materials retained some peak height for ring 1 after 40 welds.

At 100 welds, wear was more pronounced for all the electrodes. The oxide dispersion strengthened electrode C15760 showed the best performance because it retained essentially all the ring height for rings 2 through 5 after 100 welds. The other four electrode materials showed the first two rings worn completely away at 100 welds. Alloy C18000 showed the poorest performance at 100 welds with all three inner rings worn away; however, it did retain the ring structure better at 40 welds than the reference C15000 electrode.

Table 4 — Ranking of Electrode Alloy Performance Based on Pit Formation, Ring Degradation, Number of Rings Intact, and Total Amount of Ring Damage

Sheet	Least Damage				Most Damage
AA5754-O	FF19Z02	C15760	C15000 (ref)	C18150	
AA6111-T4	C15760	C18150	C18000	FF19Z02	C15000 (ref)

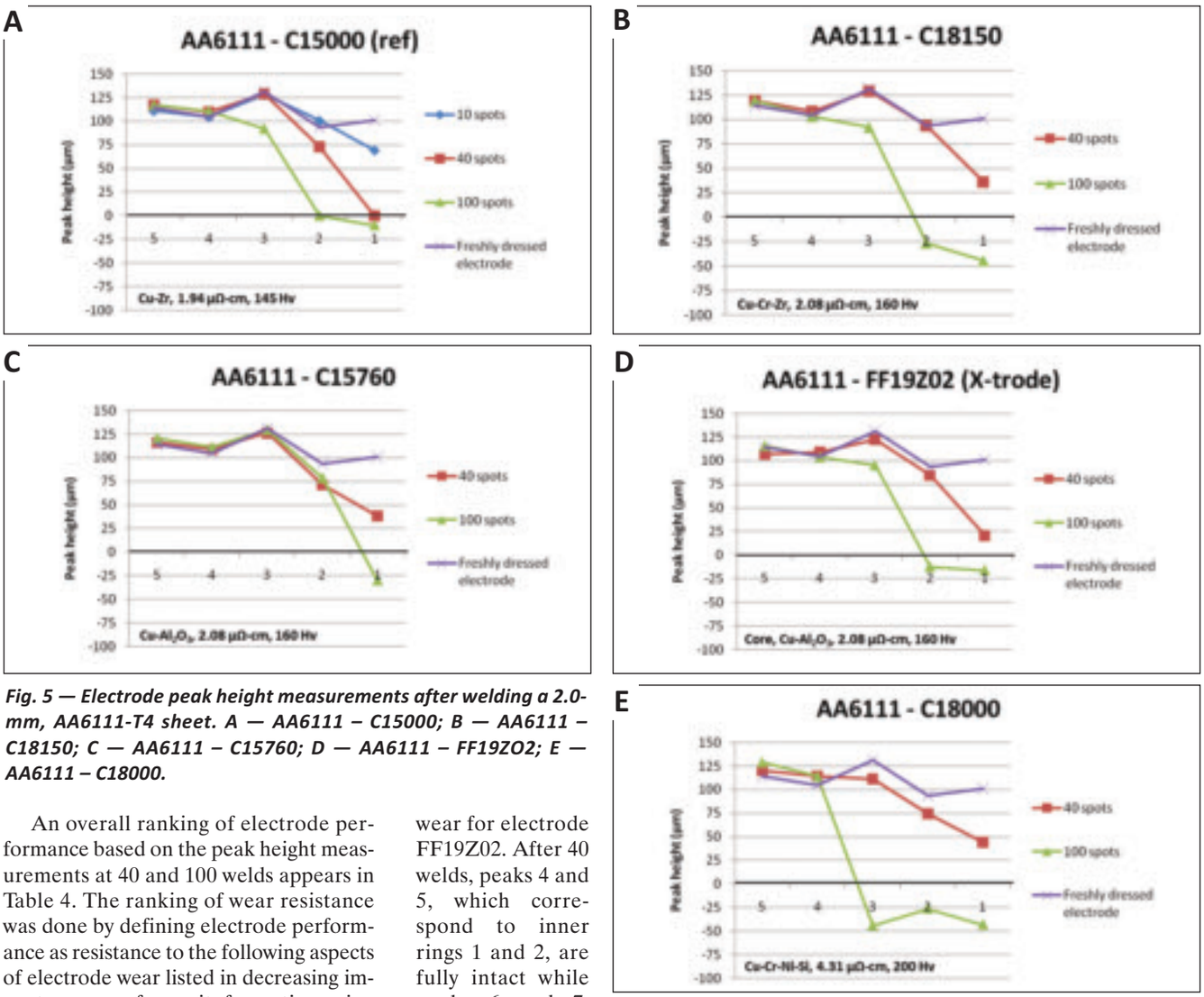

Fig. 5 — Electrode peak height measurements after welding a 2.0-mm, AA6111-T4 sheet. A — AA6111 – C15000; B — AA6111 – C18150; C — AA6111 – C15760; D — AA6111 – FF19ZO2; E — AA6111 – C18000.

An overall ranking of electrode performance based on the peak height measurements at 40 and 100 welds appears in Table 4. The ranking of wear resistance was done by defining electrode performance as resistance to the following aspects of electrode wear listed in decreasing importance: surface pit formation, ring degradation, number of rings that are intact, and total amount of ring damage.

SEM Assessment

The SEM evaluation focused on the two inner rings, numbers 1 and 2, and their surroundings. The EDS measurements were used to determine the composition of contamination layers. Because the SEM evaluation was to help explain the electrode wear mechanism by a thorough analysis of the reactions that occurred on the electrode surface, the work focused on appearance differences between the best and worst performing electrodes.

Electrodes Welding AA5754-O

To elucidate differences in wear behavior, electrodes FF19Z02 and C18150 were selected for SEM evaluation. Figure 6 shows nonsymmetrical ring wear for electrode FF19Z02. After 40 welds, peaks 4 and 5, which correspond to inner rings 1 and 2, are fully intact while peaks 6 and 7, which correspond to the opposite side of the electrode cross section, are fully worn down. These two rings (1 and 2) with their associated peaks (4, 5, 6, and 7) are located within the harder core material of the composite electrode.

Extensive buildup is also noticed on peak 6 after 40 welds (Fig. 6C and E). At 100 welds (Fig. 6B and D), pits formed at the location of the inner ring, peaks 5 and 6. All contamination found on the electrode weld face for this particular electrode/sheet combination had a composition of ~60 wt-% Cu-40 wt-% Al.

In comparison, for electrode C18150, the poorest-performing electrode of the group, SEM analysis showed heavy contamination on peak 5 after 40 spot welds. The EDS analysis at the interface between the contamination and electrode revealed a composition of ~80 wt-% Cu-20 wt-% Al. The high level of copper indicates that the aluminum diffused fairly deeply into the electrode and formed a strong metallurgical bond. The thick aluminum contamination and strong bond to the electrode surface generated extensive pitting damage to the electrode after 100 spot welds as shown by the ring height measurements in Fig. 4B (green line).

One additional electrode material was evaluated, C15760, because of its powder metallurgy structure and relatively good performance. Figure 7A and C show moderate amounts of aluminum contamination on peak 5 after 40 spot welds with an average composition ~55 wt-% Cu-45 wt-% Al. The majority of the aluminum contamination is located in the outer perimeter of peak 5.

After 100 spot welds, a large pit formed in the electrode surface at the location of peak 5, along with a crack at the bottom of the pit (Fig. 7B and D). This electrode was made using a dispersion-strengthened alloy and powder metallurgy technology, and is somewhat more

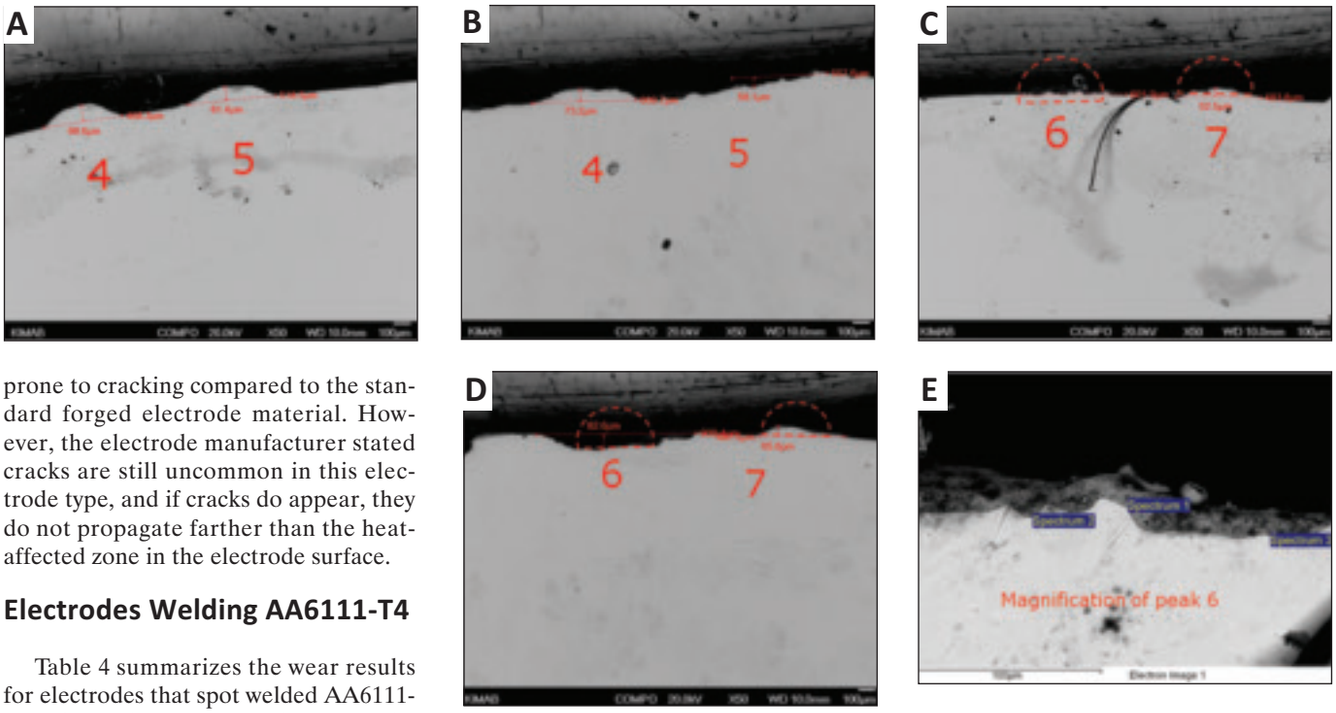

Fig. 6 — SEM images after welding AA5754-O with electrode FF19Z02. A — Peaks 4 and 5 after 40 welds; B — peaks 4 and 5 after 100 welds; C — peaks 6 and 7 after 40 welds; D — peaks 6 and 7 after 100 welds; E — higher magnification of peak 6 after 40 welds.

prone to cracking compared to the standard forged electrode material. However, the electrode manufacturer stated cracks are still uncommon in this electrode type, and if cracks do appear, they do not propagate farther than the heat-affected zone in the electrode surface.

Electrodes Welding AA6111-T4

Table 4 summarizes the wear results for electrodes that spot welded AA6111-T4. Electrodes C15760 and C15000, the best- and worst-performing electrodes, were selected for SEM evaluation.

The C15760 electrode wear is shown in Fig. 8. After 40 spot welds, only minor wear occurred on the inner ring (peaks 5 and 6) — refer to Fig. 8A and C. After 100 welds, Fig. 8B and D, wear is extensive and the inner peak is almost worn down; however, ring 2, peaks 4 and 7, is still almost intact. The contamination thickness is comparable after 40 as well as after 100 spot welds, and the composition is ~50 wt-% Cu-50 wt-% Al.

In comparison, SEM examination of the worst-performing electrode, C15000, found that peak 5 in the inner ring was fully worn down after 40 spot welds. After 100 welds, both of the two inner rings (peaks 4 and 5) were worn down, and pitting had initiated just inside of peak 5 on the electrode surface.

Electrode Ranking Analysis

Electrode wear was evaluated using several different methods. The first was visual appearance of the electrode weld face. In some situations, it was difficult to rank electrodes in terms of aluminum contamination by visual appearance, considering the electrode weld face was heavily damaged. Visual observations of contamination were more reliable early in the test, welds 10 and 40, where damage and contamination were less prevalent.

Ring height measurements were per-

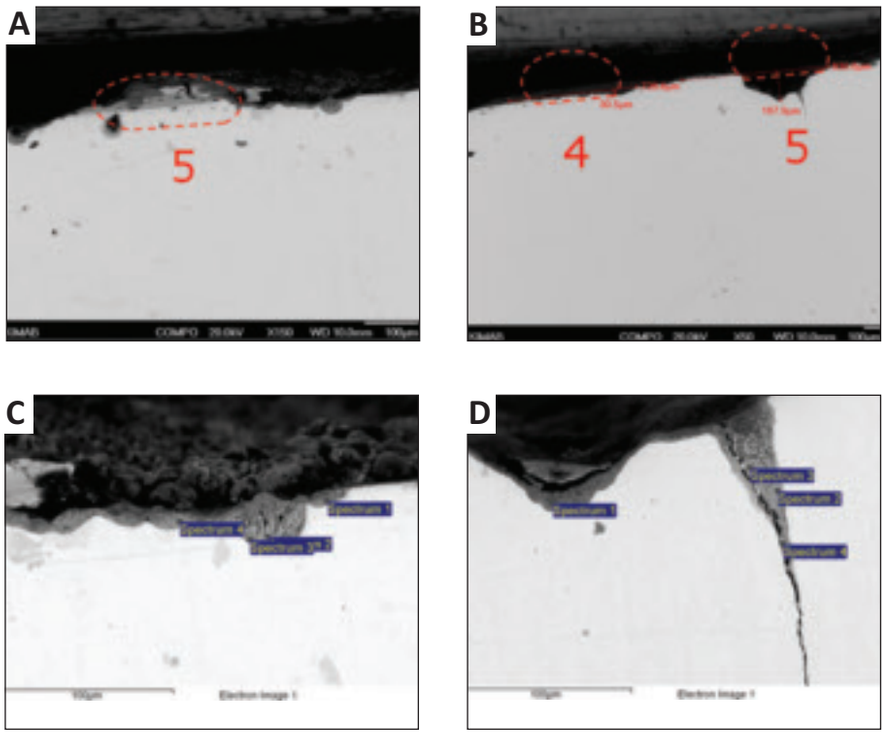

Fig. 7 — SEM images after welding AA5754-O with electrode C15760. A — Peak 5 after 40 welds; B — peaks 4 and 5 after 100 welds; C — higher magnification of peak 5 after 40 welds; D — higher magnification of peak 5 after 100 welds.

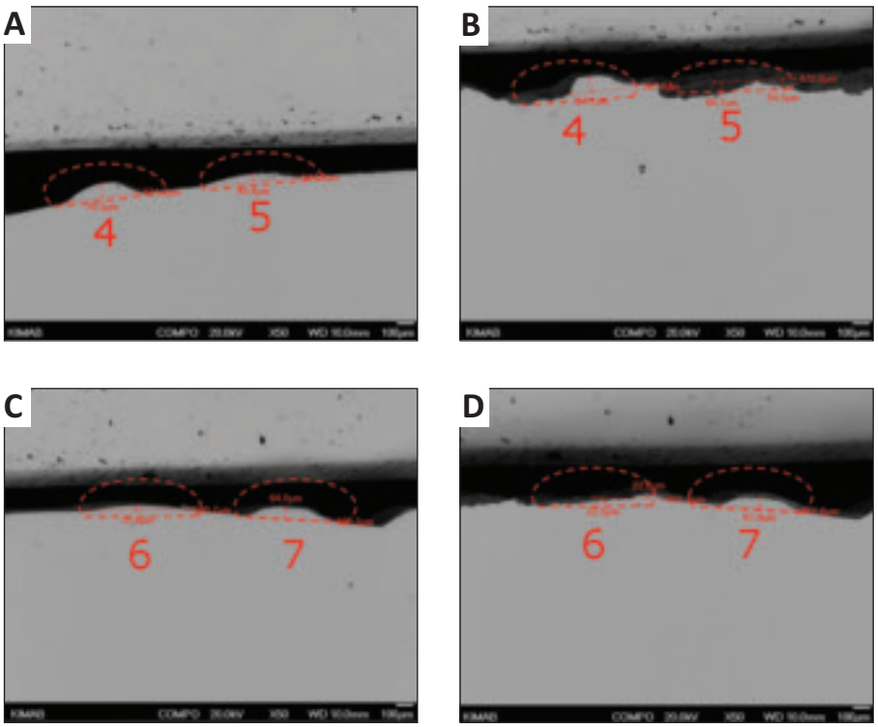

Fig. 8 — SEM images after welding AA6111-T4 with electrode C15760. A — Peaks 4 and 5 after 40 welds; B — peaks 4 and 5 after 100 welds; C — peaks 6 and 7 after 40 welds; D — peaks 6 and 7 after 100 welds.

formed as a measure of wear. The following criteria were considered to rank electrodes relative to each other in order of decreasing importance: surface pit formation, ring degradation, number of rings that are intact, and total amount of ring damage.

It was imperative to section the electrode exactly in the middle, so each electrode generated only two measurements per ring, which limits statistical validity. One solution to improve statistics would be to run multiple electrodes for one condition, but this would be too costly. A preferred method would be to complete a 3D analysis of the entire electrode weld face and ring structure; however, the technique was not available for these tests.

There appears to be little or no correlation between results from the subjective visual appearance and limited number of ring height measurements as seen in Table 5. Electrode appearance is affected by wear and contamination on the sheet surface, which is why this is not preferable as an evaluation method. Measuring the peak heights is the best evaluation method to use when classifying electrodes regarding resistance to wear.

According to the results and evaluation within this project, the optimal choice for welding AA5754-O and AA6111-T4 would be C15760, which has the highest overall performance regarding peak wear based on performance in ring height measurements.

Table 5 — Ranking of Electrode Alloy Performance Based on Visual Appearance and Ring Performance

Visual Appearance from Table 3	Ring Performance from Table 4	Visual Appearance from Table 3	Ring Performance from Table 4
AA5754-O	AA5754-O	AA6111-T4	AA6111-T4
FF19Z02	FF19Z02	C18150	C15760
C18150	C15760	FF19Z02	C18150
C15000 (ref)	C15000 (ref)	C15000 (ref)	C18000
C15760	C18150	C15760	FF19Z02
		C18000	C15000 (ref)

Electrode Wear Mechanism Highlights

Based on the findings in this study, the MRD electrode wear appears to occur in several stages as described below.

First, repeated contact of the small concentric rings against the aluminum sheet surface during spot welding causes deformation or flattening with the ring structure. This decreases their effectiveness in penetrating oxide layers on the aluminum sheet surface and causes elevated resistance at the electrode/sheet interface. As the interface resistance and interface heating rise, alloying between the copper electrode and aluminum sheet accelerates. A reaction or contamination layer builds up on the electrode weld face.

At some point, the built-up reaction layer begins to crack and spall as a response to the mechanical and thermal stresses associated with spot welding. This creates pits in the electrode surface. Thus, the wear mechanism is a combination of the rings mechanical deformation, aluminum contamination layer buildup, and finally, surface pitting caused by contamination layer spalling.

The initial wear stages are primarily mechanical damage to the ring structure, which depends upon several factors. These include the copper rings and aluminum sheet hardness, weld force, electrode weld face temperature during welding, and electrode resistance to softening. Wear can be accelerated with soft copper electrodes, hard aluminum substrates, high electrode forces, high temperatures caused by high surface resistance or excessive nugget penetration, and electrode softening during use.

Reaction between copper and aluminum is ongoing throughout the wear process. It appears to depend partly upon the alloy and surface oxides that may be present, e.g., AA5754-O with its high magnesium content and presence of Mg-containing oxides typically exhibits a more rapid contamination than AA-6111-T4. It appears to accelerate as the ring structure is deformed, because a flatter ring structure would not reduce interface resistance as effectively as newly formed rings.

Contamination results in a layer containing both copper and aluminum, most

likely as intermetallics, forming on the electrode surface. This layer is more resistive than the base copper electrode, so it will result in further heating of the electrode/sheet interface and more rapid buildup of the reaction layer. At some point in the wear process, the built-up contamination layer cracks and spalls under the action of temperature, and pressure from the spot welding process forming pits in the electrode surface.

For welding a AA6111-T4 sheet, which is harder than a AA5754-O sheet, copper hardness was considered to be a major contributing factor to maintaining the electrode ring structure. However, in the present study, the hardest electrode, C18000, did not perform best. This is attributed to the low electrical conductivity as well as the electrode's low half-softening temperature, resulting in relatively high electrode/sheet interface temperatures. This creates a different balance between mechanical deformation and surface reaction on the electrode. When the electrode weld face experiences greater heat, the metallurgical reactions between the copper electrode and aluminum sheet accelerate in relation to mechanical wear and, in turn, cause more pitting damage.

For welding softer AA5754-O sheet, almost all the electrodes tested generated extensive pitting damage on the weld face between 40 and 100 welds. The size of the pits created from welding AA5754-O was about twice as deep as those created during welding of the AA6111-T4 material. This indicates that the electrode/sheet interface attained a higher temperature during welding of the AA5754-O material as compared to AA6111-T4. This is most likely due to the thicker, more resistive Mg-containing oxides that form on the 5XXX series Al-Mg alloys. In the case of welding AA5754-O, it was difficult to distinguish which of the electrode material properties was the most important. According to our evaluation, electrodes with high half-softening temperature perform slightly better than the others.

Production Welding Details

The results of this work have a direct correlation with production welding aluminum using the MRD electrode that performs well in nonideal conditions such as welding with poor fitup (Ref. 2). This is due to the combination of a sharp radius of curvature that effectively concentrates current and ring structure on the weld face that reduces electrode/sheet interface resistance and heating.

The electrode has been found to weld satisfactorily even with fairly extensive damage (ring deformation and pit formation) to the electrode weld face. Welding to this point in production, however, would necessitate extensive dressing to restore the original weld face curvature and ring height. This would tend to shorten electrode life due to the large cut depth needed for dressing.

A more promising approach would be to dress earlier in the electrode wear process where a smaller cut depth can be used. In this case, there are a couple of options for determining at what point dressing is needed. If the rings, especially the inner rings, are fully flattened and little or no pitting has occurred, then a cut depth sufficient to recreate the rings would be sufficient. There, the cut depth would be ~0.1 mm. If minor pitting damage is visible, then slightly greater cut depths may be required. In some cases, such as welding softer 5XXX alloys, the rings may still retain some of their height. Satisfactory dressing may be obtained using smaller cut depths, such as ~0.05 mm. In this case, the electrode could provide a large number of dresses before requiring replacement.

The scenario that produces the longest electrode life will depend upon the aluminum materials to be welded, properties of the copper material used to manufacture the electrode, and welding parameters (weld force and current waveform). Extensive testing is needed to determine the process parameters that attain the longest electrode life.

Conclusions

1. Wear mechanisms for GM's MRD electrode were elucidated for RSW aluminum sheet Alloys AA5754-O and AA6111-T4. Analyses consisted of visual examination, peak height measurements, and SEM examination.

2. Based on the findings in this study, MRD electrode wear appears to occur in several steps that begin with deformation of the small concentric rings against the aluminum sheet surface. Once rings are significantly flattened, reaction accelerates between the copper electrode and aluminum sheet rapidly forming an aluminum contamination layer. Finally, as the layer thickens, it cracks and spalls under the mechanical and thermal stresses experienced during spot welding.

3. For welding Alloy AA6111-T4, electrode wear occurred primarily by ring deformation followed with eventual pit formation. This was attributed to the higher hardness of AA6111-T4 relative to annealed AA5754-O. The AA-6111-T4 sheet responded best to the high-hardness, high-conductivity electrode C15760, which would limit ring deformation without the generation of excessive heat at the electrode/sheet interface.

4. For welding Alloy AA5754-O, ring deformation was less pronounced, most likely due to the lower hardness of the sheet; however, pitting became the primary wear mechanism. This was attributed to higher electrode/sheet interface temperatures most likely caused by the Mg-containing oxides inherent on Alloys 5XXX, Al-Mg. No electrode material was preferred for welding AA5754-O aluminum.◆

Acknowledgments

The authors would like to thank Eva Lundgren of Swerea KIMAB for assisting with surface analyses. Discussions and technical support provided by Michael Karagoulis of General Motors are also greatly appreciated. Luvata is acknowledged for providing the resistance welding electrodes for evaluation.

References

1. Sigler, D. R., Schroth, J. G., and Karagoulis, M. J. Weld electrode for attractive weld appearance. U.S. Patent 8,222,560. July 17, 2012.

2. Sigler, D. R., Schroth, J. G., Karagoulis, M. J., and Zuo, D. New electrode weld face geometries for spot welding aluminum. *Conference Proceedings, AWS Sheet Metal Welding Conference XIV*, May 11–14, 2010, Livonia, Mich., pp. 1–19.

3. Sigler, D. R., and Karagoulis, M. J. Forming and re-forming welding electrodes with contoured faces. U.S. Patent Application 2010/0258536. Oct. 14, 2010.

4. Patrick, E. P., and Spinella, D. J. Surface effects on resistance spot weldability — Aluminum body sheet. *IBEC '95, Body Assembly and Manufacturing*, pp. 139–145.

5. Aluminum resistance spot welding. *GM Engineering Standards Material Specification Welding GMN3904*. March 2012.

6. Lum, I., Fukumoto, S., Biro, E., Boomer, D. R., and Zhou, Y. 2004. Electrode pitting in resistance spot welding of aluminum Alloy 5182. *Metallurgical Transactions* 35A(1): 217–226.